

PAPER • OPEN ACCESS

P-Wave and S-Wave Estimation for GPS derived seismic signal

To cite this article: A Z Sha'ameri *et al* 2019 *J. Phys.: Conf. Ser.* **1367** 012060

View the [article online](#) for updates and enhancements.



IOP | ebooks™

Bringing together innovative digital publishing with leading authors from the global scientific community.

Start exploring the collection—download the first chapter of every title for free.

P-Wave and S-Wave Estimation for GPS derived seismic signal

A Z Sha'ameri^{1,3}, S Sadiah^{1,4}, W A Wan Aris^{2,5} and T A Musa^{2,6}

¹Faculty of Engineering, School of Electrical Engineering, Universiti Teknologi Malaysia, 81310 Skudai, Johor, Malaysia.

²Faculty of Built Environment and Surveying, Universiti Teknologi Malaysia, 81310 Skudai, Johor, Malaysia.

E-mail: ³zuri@fke.utm.my, ⁴shahidatul@fke.utm.my, ⁵wananom@utm.my, ⁶tajulariffin@utm.my

Abstract. The availability of GPS (Global Positioning System) provides an alternative technology to seismography to detect earthquakes and detect their epicenters. However, the limited sampling rate and processing errors could potentially reduce the accuracy for estimating the required signal parameters. This paper evaluates the methods for analysing GPS derived seismic signals from the 2004 Sumatra Andaman Earthquake based on their time-representation, power spectrum and time-frequency representation. Between the three representations, the parameters of the earthquake signals such as P-wave and S-wave are clearly represented on the time-frequency representation.

1. Introduction

Earthquakes have so far been among the disasters recorded in the 21st-century result with the highest loss of lives at 720,113 which is about 59 percent of the total [1]. It is produced by seismic waves due to sudden release of energy in the lithosphere. Strong tremors could destroy cities and induced strong sea waves known as tsunami [2]. For that reason, the detection of an earthquake and its epicenter will provide early warning of tsunami specifically for earthquakes originating offshore. Furthermore, the information gathered is liable to assist governments to plan the future infrastructure developments and population centers and initiates contingency plans and resources in preparation for future disasters.

Besides seismography [2], alternative methods have been explored to detect earthquakes and estimate its epicenter. Among the reason highlighted is the high cost to acquire data, large amounts of data to process, and expensive equipment costs [3]. The availability of satellite technology makes Global Positioning System (GPS) an attractive alternative method. The framework of GPS based technology for earthquake detection and epicenter locating was described in [4]. Instead of directly measuring the seismic signals, the approach measures the displacement of GPS continuously operating reference stations (CORS) induced by earthquakes. The parameters of the signal derived from the displacement at multiple GPS CORS are then used for detection and estimate the epicenter location.

Among the recent work on earthquake related to GPS technology covers different analysis strategies of raw GPS measurement [5], analysis of co-seismic slip of 2014 Molucca Sea earthquake [6], analysis of peak ground velocity from earthquakes in Switzerland and Japan [7], analysis of crustal deformation associated to subduction zone and inland fault of Great Sumatran Fault (GSF) [8],



and analysis of long period signals [9]. From the work mentioned, signal analysis techniques such as power spectrum estimation was used in [7][9] and linear time-frequency representation [9] to characterize the earthquake signal. This is similar to approach to be presented in this paper. The problem of epicenter locating error was highlighted in a recent work based on the data obtained for the 2004 Sumatra Andaman Earthquake [10]. Due to the availability of GPS CORS, it would be of interest to capitalize on this technology and exploit its strength while continuously explore the processing of GPS derived seismic signals to enhance the epicenter locating. Thus, there is a need to identify the parameters from the GPS derived seismic signal to detect earthquakes and for epicenter locating.

2. Problem Statement

The low sampling rate creates difficulty to handle both satellite and receiver errors in the GPS derived seismic signals and also limits how much the true signal frequency components are captured according to the Nyquist sampling theorem. Given these limitations, it is crucial to identify the signal parameters that can be used as localization parameters for epicenter locating. Furthermore, the errors need to be understood further which could be similar to additive white Gaussian noise or narrow band Gaussian random process. Despite its disadvantages, the low sampling can still resolve the time difference between the P-wave and S-wave essential for epicenter locating using GPS CORS within far-field seismicity, which is beyond 500 km away.

3. Acquisition of GPS derived seismic signals

The availability of Global Positioning System (GPS) technology provides an alternative means to capture seismic signals. In Malaysia, GPS derived seismic signals are accessible through an existing network of GPS CORS such as the Malaysia Real-Time Kinematic Network (MyRTKnet) and National R&D CORS Network (NRC-Net) which is operated by Jabatan Ukur dan Pemetaan (JUPEM) and Universiti Teknologi Malaysia (UTM) respectively. The operation center of NRC-Net is located at Level 3, Building C02, Faculty of Built Environment and Surveying, UTM [11]. Therefore, all related research work is verifiable using real seismic signals which are ready for use without the setting up of any new infrastructure or purchase of GPS CORS. The CORS is equipped with set of geodetic type GPS/GNSS antenna and receivers that recorded raw carrier-phase measurement of dual-frequencies satellite signals L1 and L2 at 1Hz data sampling during the occurrence of 2004 Sumatra Andaman Earthquake. For the case of crustal deformation, these GPS CORS will continuously record the received signal and undergo GPS processing that include satellite orbit computation, baseline parameter estimation and realization of precise coordinate in global reference frame [6,7,8,10]. The necessary processing is required based on differencing technique, linear combination modelling and coordinate adjustment by baseline estimation to mitigate errors [10].

4. Signal Model

An earthquake event can describe in the following intervals [12]: pre-seismic (before the earthquake), co-seismic (during the earthquake) and post-seismic (after the earthquake). The GPS derived seismic signal that covers the different intervals is first sampled at f_s and the resulting signal expressed in discrete-time representation is as follows

$$\begin{aligned}
 x[n] &= a_{pre}[n] + e_{pre}[n] & N_{pre,1} \leq n \leq N_{pre,2} \\
 &= \sum_{k=0}^{\infty} a_{co,k}[n - N_{d,k}] \cos[2\pi \sum_{\lambda=-\infty}^n f_{co,k}[\lambda - N_{d,k}] + \phi_{co,k}[n - N_{d,k}]] & N_{co,1} \leq n \leq N_{co,2} \\
 &\quad + e_{co}[n] \\
 &= a_{post}[n] + e_{post}[n] & N_{post,1} \leq n \leq N_{post,2}
 \end{aligned}
 \tag{1}$$

where $a_{pre}[n]$ and $a_{post}[n]$ represent the pre-seismic and post-seismic amplitudes respectively. The amplitudes represent the displacement in millimetres the positions measured by the GPS receiver which is approximate constant. Each pre-seismic, co-seismic and post-seismic error terms $e_{pre}[n]$, $e_{co}[n]$ and $e_{post}[n]$ is modelled as zero mean Gaussian random variables is due to random and systematic errors. The co-seismic signal consists of multi-components cosine terms with amplitude $a_{co,k}[n]$, frequency $f_{co,k}[n]$ and phase $\phi_{co,k}[n]$ where each component is delayed by $N_{d,k}$. Each component of the co-seismic signal can be made to represent the sequence of signal in an earthquake starting with the P-wave, followed by the S-wave, and finally the surface wave. [2].

5. Analysis Method

Within each seismic interval defined in equation (1), the power can be calculated as follows [13]

$$P_x = \frac{1}{N} \sum_{n=0}^{N-1} |x[n]|^2 = \frac{1}{N} \sum_{n=0}^{N-1} E_x[n], \quad (2)$$

where $E_x[n]$ is the instantaneous energy and N is the interval length.

The power spectrum describes the distribution of the signal power over frequency. To obtain the power spectrum at each seismic interval, the most basic method is the periodogram which defined as [14].

$$S_x[k] = \frac{1}{N} \left| \sum_{n=0}^{N-1} x[n] e^{-j2\pi kn/N} \right|^2. \quad (3)$$

To minimize variance in the power spectrum estimate in the presence of errors, the signal is first segment and windowed before the periodogram is applied. The overall power spectrum is obtained by taking the average of all the periodogram estimated at each segment. The method described is known as the Welch method [14]. The signal $x[n]$ of length N is segmented in $L=N/DM$ sections $x_i[n]$ of length M is

$$x[n] = [x_0[n] \ x_1[n] \ x_2[n] \ \dots \ x_i[n] \ \dots \ x_{L-1}[n]] \quad (4)$$

where D is the overlap between segments (ranges from 0 to 75 percent). The periodogram calculated for each segment is [14],

$$S_{x,i}[k] = \frac{1}{MU} \left| \sum_{n=0}^{M-1} w[n-iM] x_i[n] e^{-j2\pi kn/M} \right|^2 \quad (5)$$

where $w[n]$ is a window function and U is the normalization factor defined as

$$U = \sum_{n=0}^{M-1} |w[n]|^2. \quad (6)$$

Any window function commonly used in signal processing such as the Hamming or Bartlett window function could be used. The resulting power spectrum in terms of its main lobe and spectrum leakage will depend on the selected window function. The power spectrum obtained by averaging the periodograms obtained from each segment is

$$S_{x,Welch}[k] = \frac{1}{L} \sum_{i=0}^{L-1} S_{x,i}[k] \quad (7)$$

The basic problem with the power spectrum estimation is not able to represent the temporal characteristics if the signal is time varying similar to GPS derived seismic signal. Instead of analysing the signal over the whole interval N , the power spectrum is calculated over a shorter interval M and presented over each interval in time. The resulting representation is the spectrogram which belongs to the class of quadratic time-frequency distribution. The spectrogram can be expressed as [13]

$$\rho_x[n,k] = \frac{1}{MU} \left| \sum_{\lambda=0}^{M-1} w[\lambda-n] x[\lambda] e^{-j2\pi k\lambda/M} \right|^2 \quad (8)$$

where $w[n]$ is the window function and U is the normalization factor similarly defined in the Welch method shown in equation (6).

6. Results

In this section, the analysis results are presented for the GPS derived seismic signal from the 2004 Sumatra Andaman Earthquake with the objective of estimating the P-wave and S-wave using time-representation, power spectrum and time-frequency representation. The signal is first processed in a time representation as in figure 1. Unlike the seismograph signal, the GPS derived signal are represented in three dimensions: North-South (N-S), East-West (E-W), and Vertical. The analysis results that will be presented in this section is only for N-S dimension. However, the procedure to analyze the signal is the same for all dimensions.

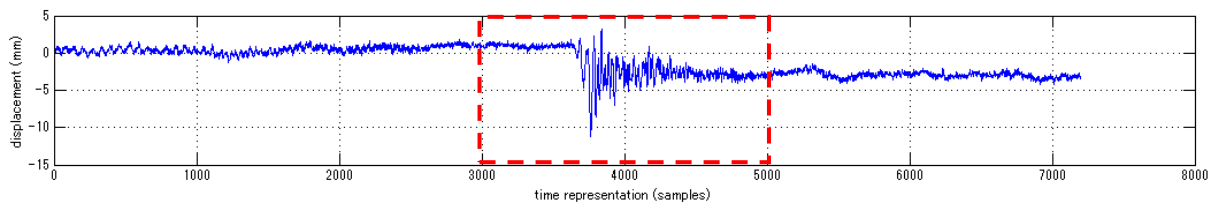


Figure 1. The captured signal in time representation for N-S dimension.

Figure 1 shows the captured signal in time representation where the horizontal axis shows the time sampled at 1 second and the vertical axis shows the displacement in millimeter. The signal is segmented into three intervals: pre-seismic (3000 – 3700 samples), co-seismic (3701 – 4200 samples) and post-seismic (4201 – 5000). The mean values are removed at each interval so that the intervals are aligned in the time-representation without the displacement as in figure 2. Note that in the analysis, the focus is on the interval between 3000th sample to 5000th sample of the overall signal which contains the seismic activity due to the earthquake.

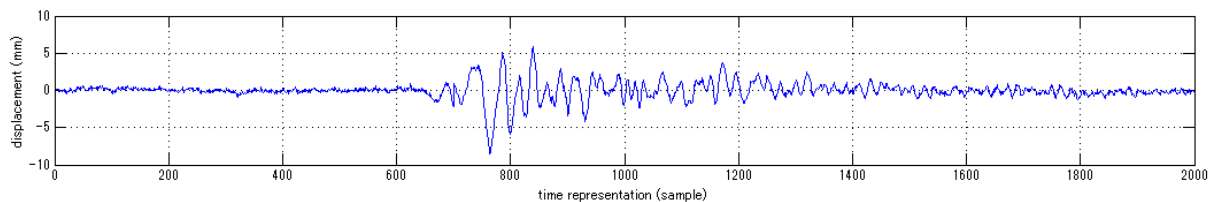


Figure 2. The overall signal after removing the mean value.

The signal after removing the mean value looks similar to seismograph signal. The next step would be to estimate the P-wave and S-wave from the time-representation which is not clearly visible. Therefore, the instantaneous energy is calculated using equation (2) producing the results in Figure 3. Two large peaks are observed during the co-seismic intervals representing the P-wave at the 761th sample, and S-wave, at the 835th sample.

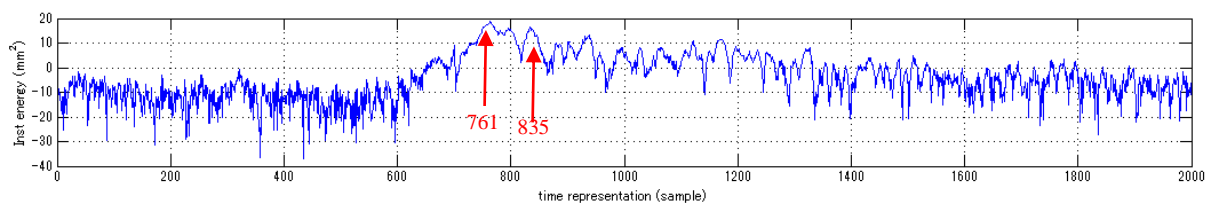


Figure 3. The instantaneous energy.

Next, the power spectrum is estimated using the Welch method described in equation (7) with the main objective of identifying the frequency contents of the signal. The resulting power spectrum shown in figure 4 does not show any specific frequency content that could be due to the P-waves and S-waves. Instead, what is observed appears to be a combination white noise (flat power spectrum) and low pass colored noise (magnitude that reduces with frequency). This is expected in the power spectrum due the receiver and satellite errors. As a conclusion, it is not possible to estimate the P-wave and S-wave from the power spectrum. The signal could be there but is hidden in the errors.

Finally, time-frequency representation is obtained using the spectrogram described in equation (8) and is shown as a contour plot in figure 5. Areas of high intensity that represents the signal power can be observed from the time-frequency representation. Two peaks observed represent the P-wave and S-wave. The first peak at the earlier time appears to be the P-wave at approximately 761 [sec] while the second peak indicates the S-wave which is approximately at 835 [sec]. The time of the two peaks is the same as what we have observed in figure 3 for the instantaneous energy. Between using time-frequency representation and instantaneous energy, the former is desirable because it provides better accuracy in presence of errors. The estimation of P-wave and S-wave is the first step to locate the epicenter of an earthquake. By taking the time difference between the P-wave and S-wave, the epicenter can be located through a process of triangulation [2].

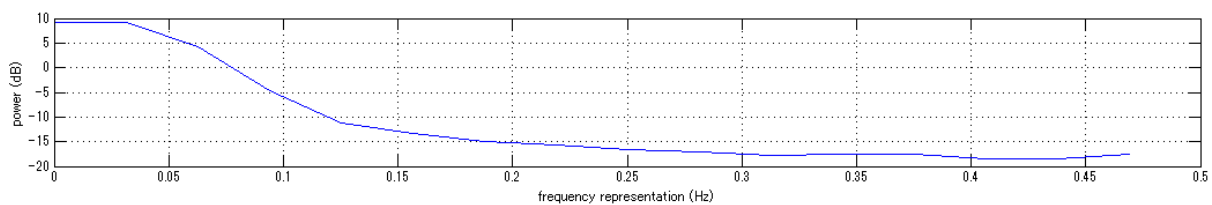


Figure 4. The power spectrum.

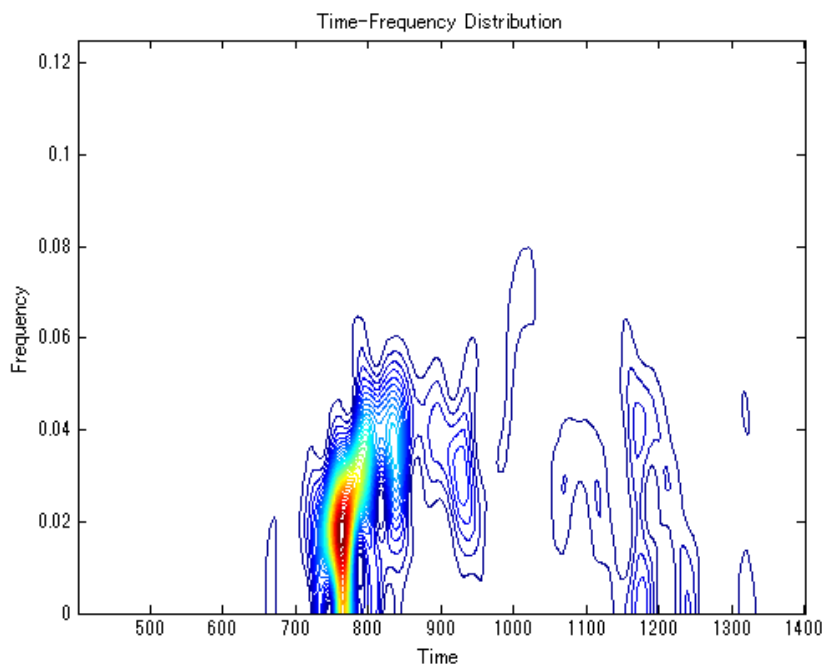


Figure 5. Time-frequency representation

7. Conclusion

Analysis of GPS derived signal from the 2004 Sumatra Andaman Earthquake shows that the P-wave and S-wave are clearly visible on the time-frequency representation compare to time representation or power spectrum estimation. The time difference between the two waves if obtained from multiple GPS CORS could be used to estimate the earthquake epicenter through a process of triangulation.

References

- [1] Disaster Death Tolls in the 21st Century, EM-DAT, CRED, International Disaster Database, <https://www.emdat.be/database>, (Last access date: 15 Feb 2019)
- [2] P. M. Shearer, 2009, Introduction to Seismology. Cambridge University Press.
- [3] Advantages and Disadvantages of Seismic Methods, Seismology: Notes, https://pburnley.faculty.unlv.edu/GEOL442_642/SEIS/NOTES/SeismicNotes02SAdv.html, (Last access date: 7 March 2019)
- [4] G. Blewitt, W. C. Hammond et al, 2009, "GPS for real-time earthquake source determination and tsunami warning systems", J Geod, Vol. 83, 2009, pp 335–343.
- [5] A. Avallone, D. Latorre et al, 2016, "Coseismic displacement waveforms for the 2016 August 24 Mw 6.0 Amatrice earthquake (central Italy) carried out from High-Rate GPS data", ANNALS OF GEOPHYSICS, 59, FAST TRACK 5; pp 1 -11.
- [6] E. Gunawan, M. Kholila I. Meilano, October 2016, "Splay-fault rupture during the 2014 Mw7.1 Molucca Sea, Indonesia, earthquake determined from GPS measurements", Physics of the Earth and Planetary Interiors Volume 259, Pages 29-33.
- [7] C. Michel, K. Kelevitz et al, June 2017, "The Potential of High-Rate GPS for Strong Ground Motion Assessment", Bulletin of the Seismological Society of America, Vol. 107, No. 3, pp. 1-11.
- [8] M. Alif, I. Meilano, E. Gunawan, 2016, J. Efendi, "Evidence of Postseismic Deformation Signal of the 2007 M8.5 Bengkulu Earthquake and the 2012 M8.6 Indian Ocean Earthquake in Southern Sumatra, Indonesia, Based on GPS Data", Journal of Applied Geodesy, Vol. 10, Issue 2.
- [9] P. Psimoulis, P. Houlié et al, 30 March - 1 Apr 2016, "Analysis of 1-Hz GPS data for the estimation of long-period surface motion of Tohoku-Oki Mw9.0 2011 earthquake", 3rd Joint International Symposium on Deformation Monitoring, Vienna, Austria.
- [10] W. A. W. Aris, 2018, Spatio-Temporal Crustal Deformation Model of Sundaland in Malaysia Using Global Positioning System, Ph. D. Thesis, Faculty of Build Environment and Survey, Universiti Teknologi Malaysia.
- [11] Senarai Lokasi Stesen Rangkaian MyRTKnet di Malaysia, The Department of Survey and Mapping Malaysia (JUPEM), http://www.data.gov.my/data/ms_MY/dataset/senarai-lokasi-stesen-rangkaian-myrtknet-di-malaysia, (Last access date: 15 Feb 2019).
- [12] Sridevi Jade, M Mukul, September 2003, "Pre-seismic, co-seismic and post-seismic displacements associated with the Bhuj 2001 earthquake derived from recent and historic geodetic data", Proc. Indian Acad. Sci. (Earth Planet. Sci.), 112, No. 3, pp. 331-345.
- [13] B. Boashash, 2015, Time-Frequency Signal Analysis and Processing 2nd Edition A Comprehensive Reference, Elsevier, Amsterdam.
- [14] J. G. Proakis, D.K. Manolakis, 2013, Digital Signal Processing, 4th Edition, Pearson.

Acknowledgment

The authors would like to thank the School of Electrical Engineering, Faculty of Engineering and the Faculty of Built Environment & Surveying, Universiti Teknologi Malaysia for providing the facilities to conduct this study.